On: 29 September 2014, At: 08:54
Publisher: Taylor & Francis
Informa Ltd Registered in England and Wales Registered Number: 1072954 Registered office: Mortimer House, 37-41 Mortimer Street, London W1T 3JH, UK

Journal of Hydraulic Research

Publication details, including instructions for authors and subscription information:
http://www.tandfonline.com/loi/tjhr20

Flow hydraulic characteristics determining the occurrence of either smooth or abrupt sewer pressurization

Giovanni B. Ferreri[a], Giuseppe Ciraolo[b] & Carlo Lo Re[c]

[a] Associate Professor, Dipartimento di Ingegneria Civile, Ambientale, Aerospaziale, dei Materiali, Università degli Studi di Palermo, Viale delle Scienze - Ed. 8 , IT-90128 Palermo, Italy

[b] Assistant Professor, Dipartimento di Ingegneria Civile, Ambientale, Aerospaziale, dei Materiali, Università degli Studi di Palermo, Viale delle Scienze - Ed. 8, IT-90128 Palermo, Italy

[c] Research Assistant Dipartimento di Ingegneria Civile, Ambientale, Aerospaziale, dei Materiali, Università degli Studi di Palermo, Viale delle Scienze - Ed. 8, IT-90128 Palermo, Italy

Published online: 15 Jul 2014.

To cite this article: Giovanni B. Ferreri, Giuseppe Ciraolo & Carlo Lo Re (2014): Flow hydraulic characteristics determining the occurrence of either smooth or abrupt sewer pressurization, Journal of Hydraulic Research, DOI: 10.1080/00221686.2014.917727

To link to this article: http://dx.doi.org/10.1080/00221686.2014.917727

IAHR AIRH
Taylor & Francis
Taylor & Francis Group

Journal of Hydraulic Research, 2014
http://dx.doi.org/10.1080/00221686.2014.917727

Research paper

Flow hydraulic characteristics determining the occurrence of either smooth or abrupt sewer pressurization

GIOVANNI B. FERRERI, Associate Professor, *Dipartimento di Ingegneria Civile, Ambientale, Aerospaziale, dei Materiali, Università degli Studi di Palermo, Viale delle Scienze - Ed. 8, IT-90128 Palermo, Italy*
Email: giovannibattista.ferreri@unipa.it (author for correspondence)

GIUSEPPE CIRAOLO, Assistant Professor, *Dipartimento di Ingegneria Civile, Ambientale, Aerospaziale, dei Materiali, Università degli Studi di Palermo, Viale delle Scienze - Ed. 8, IT-90128 Palermo, Italy*
Email: giuseppe.ciraolo@unipa.it

CARLO LO RE, Research Assistant, *Dipartimento di Ingegneria Civile, Ambientale, Aerospaziale, dei Materiali, Università degli Studi di Palermo, Viale delle Scienze - Ed. 8, IT-90128 Palermo, Italy*
Email: carlo.lore@unipa.it

ABSTRACT
Laboratory experiments showed that pipe pressurization consequent on a drastic reduction in the downstream discharge can occur either by a gradual rising of the free-surface ("smooth" pressurization) or by propagation of a front filling the whole cross-section ("abrupt" pressurization). This study examines the free-surface flow characteristics that determine smooth or abrupt pressurization pattern through a theoretical approach using dimensionless variables. A critical flow rate value, which separates the pressurization patterns, exists for any given pipe diameter. For flow rates higher than this specific value, only abrupt pressurization occurs. For lower flow rates, either smooth or abrupt pressurization can take place; smooth pressurization occurs when the free-surface flow depth falls within a specified range, depending on the flow rate itself and the pipe diameter, whereas abrupt pressurization occurs when the depth falls outside this range. The comparison with actual uniform-flow conditions allows one to predict the pressurization pattern and the related pipe surcharge (in the case of abrupt pressurization). The analysis also shows that, in practice, severe surcharges can be expected even in the case of only partial reduction of the downstream discharge.

Keywords: Pressurization; storm sewer system; transition; unsteady flow; urban drainage

1 Introduction

Sewer pressurization is a frequent phenomenon occurring in urban drainage networks as a consequence of storms, even if these events are not exceptional. Pressurization can generate high pressure oscillations that can raise or even eject manhole covers (Hamam and McCorquodale 1982, Guo and Song 1991) and sometimes form geysers (i.e. intermittent air–water jets in the atmosphere) (Guo and Song 1990, 1991), or even severely damage sewers (Hamam and McCorquodale 1982, Zhou *et al.* 2002a). Despite these potential drawbacks, the phenomenon has not been extensively explored; however, it has been established that intense and frequent pressure oscillations observed in experiments carried out in a variety of conditions are caused by the complex interaction between water flow and air pockets entrapped in pipes and manholes (Hamam and McCorquodale 1982, Zhou *et al.* 2002b, Vasconcelos and Wright 2005, Ferreri *et al.* 2014). Moreover, various experiments have shown that the amount of entrapped air and the air pocket arrangement inside the water flow depend on the pipe pressurization pattern.

Pressurization can proceed from upstream due to an increase in the pipe inflow, or from downstream due to a decrease in the pipe outflow, which has been studied more extensively. A decrease in the pipe outflow, in practice, may arise from malfunctions of the storm sewer system, such as back flow from the downstream pipe, total or partial obstruction of the downstream pipe, pump stoppages, or other problems. Drastic and rapid reduction of pipe outflow has been investigated experimentally by several researchers who detected three pressurization patterns.

Received 18 April 2013; accepted 20 April 2014/Currently open for discussion.

ISSN 0022-1686 print/ISSN 1814-2079 online
http://www.tandfonline.com

In the first pattern (studied by Capart *et al.* 1997, Trajkovic *et al.* 1999, Ferreri *et al.* 2014), the bore caused by the closing operation in the downstream tank did not reach the pipe crown, and the pipe pressurization occurred because of a gradual rise in the flow free-surface. In the second pattern (studied by Hamam and McCorquodale 1982, Cardle *et al.* 1989) the bore completely filled the pipe cross-section because the pressure head exceeded the pipe crown, and the travelling bore caused free-surface instability that rose until reaching the pipe crown. In this pattern, filling ratios were higher than 0.8 (i.e. the instability limit for circular pipes), and an air pocket was entrapped between the advancing bore and the wave caused by instability; the air–water interaction then yielded pressure oscillations. The third pattern (Ferreri *et al.* 2014) involved filling ratios lower than 0.8. In this pattern, the bore completely filled the pipe cross-section but, in contrast to the second pattern, no free-surface instability occurred; however, due to progressive air entrainment as the bore travelled, air pockets formed inside the water flow, which produced intense pressure oscillations as they were released through the upstream tank. Air pockets could be large or small, depending on the flow characteristics.

Each pattern generated pressure oscillations having different characteristics, such as start time, intensity, and duration; therefore, prediction of the pattern in addition to the occurrence of pressurization is an important practical issue. Despite this, no specific studies are available in the technical literature, and consequently no criteria exist for predicting the bore characteristics.

To expand knowledge on pressurization, we conducted experiments on a wider range of pipe slopes, flow velocities, and filling ratios than addressed in previous studies. Details on the experimental equipment, the run characteristics, and the major results are in Ferreri *et al.* (2014). In the runs, pipe pressurization occurred following either the first or the third pattern, called, respectively, "smooth" and "abrupt" pressurization. Note that the second pattern (not observed in these experiments) is a particular implementation of abrupt pressurization that occurs as the filling ratio exceeds 0.8. Numerical examination of the transient characteristics and pressure oscillations was carried out by Ferreri *et al.* (2010) for smooth pressurization and by (Ciraolo and Ferreri 2008a, 2008b) for abrupt pressurization. The flow characteristics (flow rate and flow depth) that determine the occurrence of a smooth or abrupt pattern are addressed in this paper. The problem was examined theoretically with dimensionless variables to obtain general results. Through the analysis of an *ad hoc* novel abacus, the actual situations of flow and pipe characteristics were detected, and the occurrence domain of each of the two pressurization patterns was bounded in the abacus itself.

2 Experimental results

The experiments were carried out in a tilting circular pipe between two steel tanks having an internal diameter $D = 244$ mm. The transient water flow was initiated by the sudden closing of a sluice-gate at the downstream tank outlet located on the lower part of the wall opposite the pipe end. The wall could be located in three positions, *A*, *B*, and *C*, at about 29, 14.5, and 0 cm, respectively, from the pipe end. The changeable wall position was designed to investigate whether the tank capacity affected the transient flow characteristics.

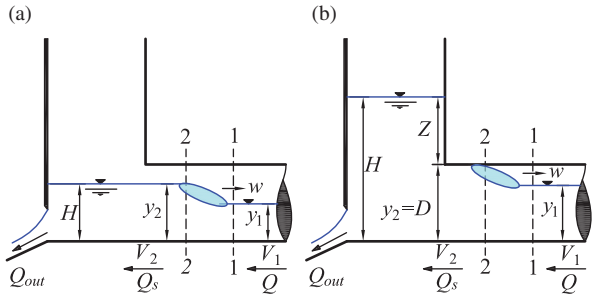

Figure 1 Water level in the downstream tank and formation of the bore front for (a) smooth and (b) abrupt pressurization

The experimental runs included 48 combinations of pipe slope and flow rate for each movable wall position, totalling 144 runs. The free-surface flow characteristics ranged as follows: pipe slope $S_0 = 0.2$–2.5%, flow rate $Q = 15$–$65\ \mathrm{dm^3\ s^{-1}}$, filling ratio $y_1/D \approx 0.3$–0.8 (y_1 being the flow depth), velocity $V_1 \approx 0.79$–$2.8\ \mathrm{m\ s^{-1}}$, and Froude number $\mathsf{F}_1 \approx 0.7$–3, which was computed by $\mathsf{F}_1 = V_1/\sqrt{gA_1/B_1}$, where A_1 is the cross-sectional area, B_1 the free-surface width, and g the gravity acceleration.

For the lower flow rates, the bore produced by the closing operation did not reach the pipe crown (Fig. 1a), and its migration along the pipe caused the free-surface to rise without touching the pipe crown. After the front passed, as the downstream tank filled the free-surface began to rise gradually, thus causing *smooth* pipe pressurization beginning from the downstream end. As the flow rate increased, the bore height grew along with the level in the downstream tank, which first reached and then went over the pipe crown (Fig. 1b). Consequently, the bore completely filled the pipe cross-section, and therefore each pipe cross-section experienced *abrupt* pressurization as it was reached by the front.

Smooth pressurization was observed in the runs having flow rates $Q \leq 20\ \mathrm{dm^3\ s^{-1}}$, which were tested only with the two lowest pipe slopes ($S_0 = 0.2\%$ and 0.6%), whereas abrupt pressurization was observed in the runs having $Q \geq 25\ \mathrm{dm^3\ s^{-1}}$, which included all six pipe slopes considered ($S_0 = 0.2\%, 0.6\%, 1.0\%, 1.5\%, 2.0\%$, and $2.5\ \%$). From these results the following questions arise: (1) did a sole discriminant flow rate between 20 and $25\ \mathrm{dm^3\ s^{-1}}$ exist irrespective of the pipe slope and (2) would other physical conditions affect the occurrence of one of the two pressurization patterns. These questions were answered using a mathematical approach.

3 Mathematical approach

3.1 *Tank filling and front formation*

For the mathematical treatment of tank filling and front formation, the following assumptions were made (see Fig. 1): (1) the

free-surface flow coming from the upstream tank (flow rate Q) has uniform-flow conditions with velocity V_1 and cross-sectional area A_1; (2) the pipe is horizontal, and its invert is aligned with the tank bottom; (3) the downstream tank is ventilated so that pressure on the free-surface is always equal to atmospheric pressure; (4) pressure distribution in the downstream tank and in each pipe cross-section is hydrostatic; and (5) the height, H, of the tank water level equals the pipe invert pressure head in Section 2 (i.e. downstream of the moving jump); as long as the pipe does not pressurize, H is equal to the sequent depth y_2 but, as the pipe pressurizes, it is equal to the pipe diameter D increased by the surcharge Z. Tank filling is ruled by the continuity equation

$$\Sigma \frac{dH}{dt} = Q_s - Q_{out} \tag{1}$$

where Σ is the tank horizontal section; $Q_s = V_2 A_2$ is the flow rate in Section 2 that enters the tank; V_2 and A_2 are the flow velocity and flow cross-sectional area in Section 2, respectively; Q_{out} is the tank outflow; and t is the time. If $H < D$ (Fig. 1a) then $A_2 = A(y_2)$, whereas if $H > D$ (Fig. 1b) then $A_2 = \pi D^2/4$. For the moving hydraulic jump, the continuity and the momentum equations must be considered. With respect to a reference integral with the bore front migrating upstream with absolute celerity w, the continuity equation for the control volume between Sections 1 and 2 gives

$$(V_1 + w)A_1 = (V_2 + w)A_2 \Rightarrow w = \frac{V_1 A_1 - V_2 A_2}{A_2 - A_1} \tag{2}$$

Again, with respect to the reference integral with the front, neglecting the sum of the flow resistance and weight component, the momentum equation along the flow direction for the same control volume, after manipulations taking Eq. (2) into account (here omitted for the sake of brevity), gives

$$g(y_{G1}A_1 - y_{G2}A_2) + (V_1 - V_2)^2 \frac{A_1 A_2}{A_2 - A_1} = 0 \tag{3}$$

where y_{G1} and y_{G2} are the pressure heads in the centroids of Sections 1 and 2, respectively (Fig. 1). If $H < D$ (Fig. 1a) then y_{G2} is the centroid dip under the free-surface, whereas if $H > D$ (Fig. 1b) then $y_{G2} = H–D/2$.

Four simulations of tank filling relating to the experimental flow rate $Q = 20\,\mathrm{dm^3\,s^{-1}}$ with the measured V_1 and A_1 values (sub-critical flow) were conducted (Fig. 2); total and instantaneous closing of the tank gate was assumed ($Q_{out} = 0$), and the initial water level in the tank was the same as in the pipe (i.e. $H_0 = y_1$). The simulations related to the experimental positions of the movable wall A, B, and C in addition to a hypothetical position E located at 60 cm. For all the positions, the water level quickly reaches the same maximum height, which is consistent with the experimental evidence that the front height did not depend on the location of the movable wall. In practice, the tank height would begin to increase as the propagating bore

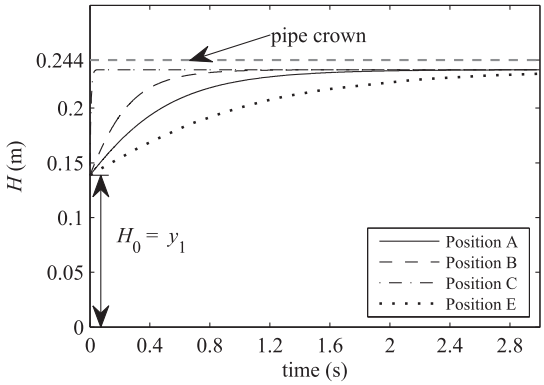

Figure 2 Tank filling for positions A, B, C, and E of the wall opposite to the pipe end, located, respectively, 29, 14.5, 0.5, and 60 cm from the pipe end

flows into an upstream tank, as the experimental runs confirmed. However, the very short time for the maximum height to be reached implies that the bore propagation does not practically affect the front height. The slight decrease of the front height revealed in the experiments was caused by the pipe slope, here assumed equal to zero. Therefore, the front height is the same as produced by instantaneous closing at the end section of the pipe (zero tank capacity). This is the operation we considered to determine the head at the pipe end, assumed equal to the tank level H; consequently, the following equality occurs instantaneously:

$$V_2 A_2 = Q_{out} \tag{4}$$

3.2 *Flow conditions discriminating smooth from abrupt pressurization*

Equation (3) gives

$$V_1 = V_2 + \sqrt{-g(y_{G1}A_1 - y_{G2}A_2)\frac{A_2 - A_1}{A_1 A_2}} \tag{5}$$

from which

$$Q = \frac{Q_{out}A_1}{A_2} + A_1\sqrt{-g(y_{G1}A_1 - y_{G2}A_2)\frac{A_2 - A_1}{A_1 A_2}} \tag{6}$$

Setting $Q_{out} = \psi Q$ (with $0 \le \psi < 1$), Eq. (6) becomes

$$Q = \frac{A_2}{A_2 - \psi A_1}A_1\sqrt{-g(y_{G1}A_1 - y_{G2}A_2)\frac{A_2 - A_1}{A_1 A_2}} \tag{7}$$

For fixed Q and ψ (i.e. Q_{out}), Eq. (7) allows H to be determined for a given y_1 or vice versa. The free-surface flow conditions discriminating smooth from abrupt pressurization, for a fixed ψ, are obtained from Eq. (7) setting $H = y_2 = D$ (i.e. $A_2 = \pi D^2/4$; $y_{G2} = D/2$), which gives a relationship between Q and y_1 only.

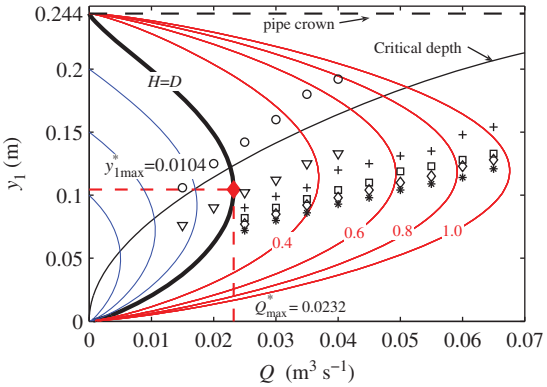

Figure 3 Relationship $Q - y_1$ for a few tank heads H and disposition of the points relating to the experimental combinations

In the case of $Q_{out} = 0$ studied experimentally in Ferreri *et al.* (2014), Eq. (7) becomes

$$Q = A_1\sqrt{-g(y_{G1}A_1 - y_{G2}A_2)\frac{A_2 - A_1}{A_1A_2}} \tag{8}$$

The discriminant flow conditions are represented by the "limit curve" (thick line in Fig. 3), which shows that there is a maximum flow rate, Q^*_{max}, that may produce a tank head $H = D$, provided the free-surface flow depth is just $y^*_{1,max}$. For lower flow rates, only the two depths y_1 given by the curve allow the tank head to be $H = D$, whereas for higher flow rates the head will be $H > D$.

Figure 3 also shows a few curves relating to values of $H < D$ (smooth pressurization), a few curves relating to values of $H > D$ (abrupt pressurization) and the curve of critical depth y_c expressed by

$$Q = A_c\sqrt{g\frac{A_c}{B_c}} \tag{9}$$

where A_c and B_c are the cross-sectional area and the free-surface width relating to the critical depth, respectively. Each curve relating to parameter H has a maximum flow rate $Q_{max,H}$ for which the tank head equals the parameter H itself; $Q_{max,H}$ increases along with H. All curves relating to smooth pressurization are inside the domain bounded by the y_1-axis and the limit curve, whereas all the curves relating to abrupt pressurization are inside the domain bounded by the Q-axis, the straight line $H = D$ and, on the left, by the limit curve. The points representing the 48 experimental combinations are also reported, and their localization in the two domains confirms the experimental results: only the points relating to $Q \leq 20\,\mathrm{dm^3\,s^{-1}}$ are inside the domain of smooth pressurization. Note that the occurrence of smooth or abrupt pressurization is not determined by the sub-critical or super-critical condition of the early free-surface flow; moreover, the maxima of the curves are always below the critical-depth curve.

The maximum of each curve is obtained by zeroing the derivative of Eq. (7), which after several manipulations yields

$$A_2\frac{B_1}{A_1^2}(y_{G1}A_1 - y_{G2}A_2)\frac{A_2 - A_1(2-\psi)}{A_2 - \psi A_1} + (A_2 - A_1) = 0 \tag{10}$$

where B_1 is the width of the free-surface in Section 1. Setting $\psi = 0$ and $y_2 = D = 0.244\,\mathrm{m}$, Eq. (10) gives $y^*_{1,max} = 0.104\,\mathrm{m}$ and $Q^*_{\max} = 23.2\,\mathrm{dm^3\,s^{-1}}$, a value consistent with our experimental results.

For a generic ψ value ($Q_{out} \neq 0$), curves analogous to those reported in Fig. 3 are obtained; obviously, for a given H value these curves present as higher maximum flow rates as higher ψ values (see the following section).

3.3 *Analysis through dimensionless variables*

To obtain general quantitative results, the above treatment was developed using the following dimensionless variables (Fig. 4):

$$\eta = \frac{y}{D}; \quad h = \frac{H}{D}; \quad \alpha = \arccos(1-2\eta);$$
$$a = \frac{A}{D^2} = \frac{1}{4}(\alpha - \sin\alpha\cos\alpha); \quad b = \frac{B}{D} = \sin\alpha;$$
$$p = \frac{P}{D} = \alpha; \quad r = \frac{R}{D} = \frac{a}{\alpha};$$
$$\eta_G = \frac{y_G}{D} = \frac{1}{2}\left[\frac{2\sin^3\alpha}{3(\alpha - \sin\alpha\cos\alpha)} - \cos\alpha\right];$$
$$q = \frac{Q}{(gD^5)^{1/2}};$$
$$v = \frac{V}{(gD)^{1/2}}; \quad \nu = n\frac{g^{1/2}}{D^{1/6}} \tag{11}$$

where η is the filling ratio, P is the wet perimeter, R is the hydraulic radius, and n is the Manning's roughness coefficient. Introducing the variables (11), Eqs. (7), (9), and (10) become, respectively

$$q = \frac{a_2}{a_2 - \psi a_1}a_1\sqrt{-(\eta_{G1}a_1 - \eta_{G2}a_2)\frac{a_2 - a_1}{a_1a_2}} \tag{12}$$

$$q = a_c\sqrt{\frac{a_c}{b_c}} \tag{13}$$

$$a_2\frac{b_1}{a_1^2}(\eta_{G1}a_1 - \eta_{G2}a_2)\frac{a_2 - a_1(2-\psi)}{a_2 - \psi a_1} + (a_2 - a_1) = 0 \tag{14}$$

whereas the normal flow equation is

$$q = v\,a = \frac{S_0^{1/2}}{\nu}r^{2/3}a = \theta\,r^{2/3}a \tag{15}$$

where S_0 is the pipe slope and $\theta = S_0^{1/2}/\nu$; as $h \geq 1$, $a_2 = \pi/4$, and $\eta_{G2} = (h - 1/2)$.

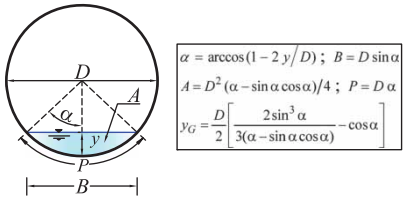

Figure 4 Sketch of the pipe cross-section and expressions used

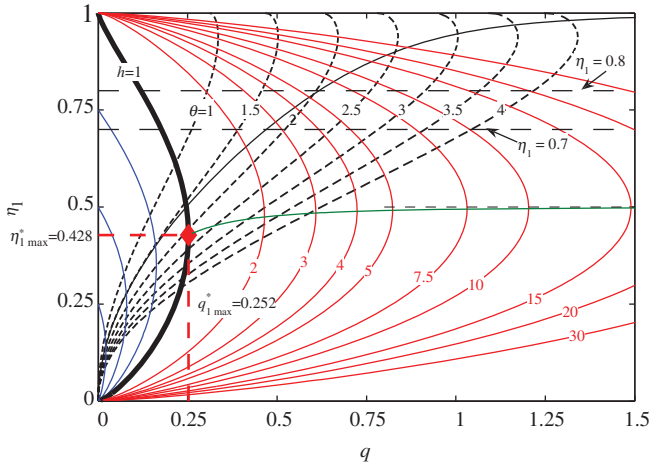

Figure 5 Representation of the relationship between flow rate q, free-surface flow depth η_1, and tank head h, contextualized with actual uniform-flow curves having a parameter θ and critical-flow curve; the curve linking the maxima and its asymptote are also shown

For the experimental case $Q_{out} = \psi = 0$, the curves obtained by Eq. (12) for a few values of the parameter $h = 0.25$–30 (i.e. $H = 0.25$–$30D$) are reported in Fig. 5; the limit curve is that having $h = 1$, whose maximum dimensionless flow rate is $q^*_{max} = 0.252$ for the filling ratio $\eta^*_{1,max} = 0.428$. The figure also shows the curve linking the maxima of the family of curves having $1 \le h \le 30$, whose equation is

$$q_{max,h} = a_1 \frac{a_2 - a_1}{a_2 - \psi a_1} \sqrt{\frac{a_2 - \psi a_1}{a_2 - a_1(2-\psi)} \frac{a_1}{b_1}} \qquad (16)$$

which is obtained by eliminating $(\eta_{G1} a_1 - \eta_{G2} a_2)$ between Eqs. (12) and (14). However, as h increases, the related filling ratio for the maximum flow rate, $\eta_{1,max,h}$, tends asymptotically to the value 0.5, which is easily obtained from Eq. (16) observing that as $a_1 \to a_2/(2-\psi)$, there follows $q_{max,h} \to \infty$. Therefore, for practical purposes, a rough but effective assessment of the maximum flow rate $q_{max,h}$ relating to $h \ge 1$ can be obtained by setting $\eta_1 = 0.5$ in Eq. (12).

To predict practical situations where smooth or abrupt pressurization occurs, several curves of uniform-flow (Eq. 15) are also reported (Fig. 5) relating to values of $\theta = S_0^{1/2}/\nu$ between 1 and 4. This range includes most of the practical situations, as indicated by a few examples reported in Table 1, where V_{70} is the flow velocity for the filling ratio $\eta = 70\%$: the lowest θ values concern large tunnels, whereas the highest values concern small diameter sewers. Finally, the lines $h = 0.7$ and $h = 0.8$ bound the range of filling ratios usually adopted in sewer design; note that over the $h = 0.8$ limit, sewers may pressurize suddenly because of free-surface instability (Hamam and McCorquodale 1982, Cardle *et al.* 1989).

Table 1 Examples of $S_0^{1/2}/\nu$-values for a variety of actual situations

D (m)	n (s m$^{-1/3}$)	S_0	V_{70} (m s^{-1})	$S_0^{1/2}/\nu$
0.25	0.014	0.05	2.82	4.05
0.5	0.013	0.02	3.05	3.09
1	0.013	0.02	4.83	3.47
2	0.013	0.005	3.84	1.95
5	0.011	0.002	5.28	1.70
10	0.011	0.0006	4.59	1.04

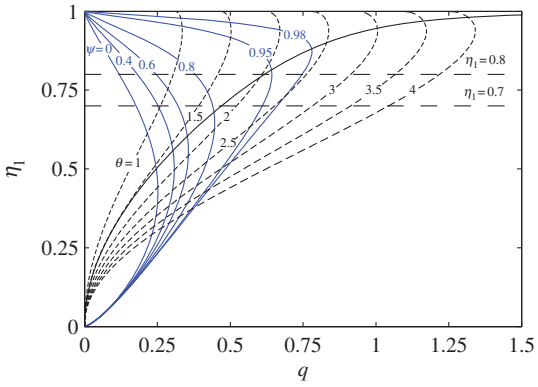

Figure 6 Dimensionless limit curves for various ψ-values

In practical situations a discharge $Q_{out} \ne 0$ is likely. The limit curves ($h = 1$; Eq. 12) relating to a few values of $\psi = Q_{out}/Q$ are compared in Fig. 6. The figure also reports the uniform-flow curves, the critical-depth curve and the lines $h = 0.7$ and $h = 0.8$. As the discharged flow rate increases, the domain of smooth pressurization noticeably expands (i.e. the value of q^*_{max} increases noticeably), but practical situations causing abrupt pressurization continue to occur; for a given η_1, the higher is the ψ-value, the larger are the θ-values for which abrupt pressurization occurs. Information on the h-values reached for a fixed discharge q_{out} are given in Fig. 7, where, for a few ψ values, several curves having a parameter h are reported.

As ψ increases (i.e. Q_{out} increases) the practical possibility to reach high h-values considerably shrinks (Fig. 7); however, noticeable h-values can be generated for ψ-values lower than 0.5. For each ψ-value, the curve linking the maxima of the family of curves having a parameter $h \ge 1$ is expressed by Eq. (16); nevertheless, a rough assessment of $q_{max,h}$ is given by Eq. (12) assuming for η_1, analogously to the case $\psi = 0$, the solution of

$$a_1 = \frac{a_2}{(2-\psi)} \qquad (17)$$

for all h-values.

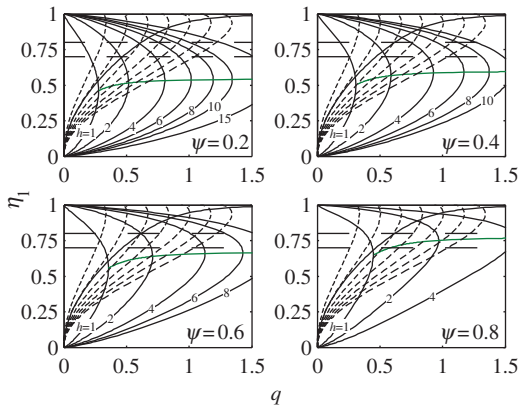

Figure 7 Comparison among the curves $q(\eta_1)$ for fixed h-values related to a various ψ-values

4 Discussion

The results demonstrate that, in extreme case of $Q_{out} = 0$ ($\psi = 0$), both smooth and abrupt pressurization can occur in practical situations, depending on the position of dimensionless flow rate and flow depth of the early free-surface flow with respect to the limit curve described by Eq. (12) (Fig. 5). For a flow rate $q < q^*_{max}$, two relative depths, η_1, would theoretically allow the relative tank head to be $h = 1$ (i.e. $H = D$); the lower depth is always of super-critical flow, whereas the higher depth is either of super-critical flow or sub-critical flow, depending on the position of q with respect to the value $q_{l,c} = 0.246$ for which the critical-flow curve intersects the limit curve.

Assuming that in practical cases uniform-flow conditions occur, the disposition in the plane of the sheaf of actual uniform-flow curves shows that the limit condition, $H = D$, occurs with a sub-critical flow only for $S_0^{1/2}/\nu < 1.58$ (i.e. the value for which the uniform-flow curve passes through the intersection point between the limit curve and the critical-flow curve). Therefore, assuming a design velocity V_{70} of about 5 m s^{-1}, according to Eq. (15) the occurrence of the limit condition with a sub-critical flow (mild slope) will only concern tunnels having a diameter $D \geq 5$ m, whereas for lower diameters the limit condition will occur with a super-critical flow (steep slope).

If we consider that drainage conduits are usually designed to operate with a filling ratio $\eta_1 = 0.70$–0.80, a tank head up to $H = 2D$ can be predicted for $\theta = 1$ (largest diameters), whereas for $\theta = 4$ (smallest diameters) even heads up to $H = 10$–$20D$ can occur (Fig. 5), which may cause immediate ejection of the manhole cover as the front forms (i.e. before the pipe pressurizes and air pockets are entrapped).

High tank heads can be generated in the case of a partial reduction of the discharged flow rate (i.e. $Q_{out} \neq 0, 0 < \psi < 1$); however, the higher ψ the higher q-values causing such high heads. In the usual design range, $\eta_1 = 0.70$–0.80, values up to $\psi = 0.4$ for all the considered actual situations (i.e. $1 \leq \theta \leq 4$) cause abrupt pressurization (Fig. 7). Abrupt pressurization actually occurs even for $\psi = 0.8$ (i.e. a reduction in the flow rate Q_{out} by only 20%) in all the situations relating to $\theta \geq 1.69$, which involves most actual conduits. The comparison of the four panels (Fig. 7) shows that, for the smaller diameters ($\theta = 3.5$–4), h can range between ≈2 and ≈8 for $\psi = 0.8$ and 0.2, respectively.

Even higher heads than those related to the usual design filling ratios, can occur when, as a consequence of extreme rainfalls, the filling ratio exceeds 0.8 without the pipe pressurizing because of free-surface instability. In such a case, a rapid drop in the tank discharge, Q_{out}, down to almost zero, may cause theoretical tank heads up to 30 times the diameter or more (Fig. 5). These high heads decrease in the case of a partial reduction in the flow rate discharged (Fig. 7), but they remain considerably higher than those of the usual design range.

By contrast, lower tank heads than those related to the design filling ratios can be reached for yearly floods because they flow with markedly lower filling ratios, as shown by our experiments. Even floods flowing with filling ratios noticeably lower than 0.5 can still generate abrupt pressurization; the relating head value depends on the ψ-value and the filling ratio η_1.

The high heads generated by abrupt pressurization suggest that undesired events such as ejection of manhole covers and sewer damages may arise, not only from intense pressure oscillations produced by the interaction between entrapped air pockets and water flow (Zhou *et al.* 2002a, Vasconcelos and Wright 2005, Ferreri *et al.* 2014), but also from the formation process of the bore front in the downstream manhole. Note that in case of unvented manhole covers, both air already present in a given manhole and air captured by the bore cannot flow out from the manhole itself. Dynamic interaction between entrapped air and water flow may subsequently result in considerably higher surcharges than for well-ventilated drainage systems, as considered in this study. This interaction concerns both the manhole where the bore forms and the manholes run across by the propagating bore.

5 Conclusions

Mathematic treatment confirmed experimental evidence that consequent pipe pressurization on total or partial sudden closing of the downstream tank outlet can occur by either (1) gradual rising of the flow free-surface (smooth pressurization) or (2) propagation of a bore filling the whole pipe cross-section (abrupt pressurization). In particular, for a fixed ratio between the downstream tank outflow and the pipe flow rate, a maximum flow rate exists depending on the pipe diameter only, for which smooth pressurization can occur. For higher flow rates, only abrupt pressurization can occur, whereas for lower flow rates the pressurization pattern (smooth or abrupt) is actually determined by the free-surface flow depth. Both patterns can occur with both sub-critical and super-critical flow.

In the case of abrupt pressurization with zero tank outflow, for the usual design filling ratios (0.7–0.8) a surcharge up to about one diameter for the largest tunnels (10 m diameter or more) and up to about 20 diameters for the smallest sewers (a few decimetres

diameter) can be expected. Considerable surcharge is expected even with a non-zero tank outflow, but it noticeably decreases as the outflow increases.

Abrupt pressurization can occur in practical situations even for flow depths less than half a diameter, which implies that abrupt pressurization can happen not only for "extreme" floods (flowing with filling ratios higher than 0.7), but also for yearly floods.

The possibility that considerable heads can be generated during the formation of the bore further explains manhole cover ejection and sewer damage during rainfall events.

Notation

A = flow cross-sectional area
A_1 = free-surface flow cross-sectional area in Section 1 (m^2)
A_2 = flow cross-sectional area in Section 2 (m^2)
A_c = critical-flow cross-sectional area (m^2)
a = dimensionless cross-sectional area A (–)
a_1 = dimensionless cross-sectional area A_1 (–)
a_2 = dimensionless cross-sectional area A_2 (–)
a_c = dimensionless cross-sectional area A_c (–)
B = free-surface width (m)
B_1 = free-surface width in Section 1 (m)
B_c = free-surface width for critical flow (m)
b = dimensionless free-surface width B (–)
b_1 = dimensionless free-surface width in Section 1 (–)
b_c = dimensionless free-surface width for critical flow (–)
D = pipe diameter (m)
F_1 = free-surface flow Froude number in Section 1 (–)
g = gravity acceleration ($m\,s^{-2}$)
H = tank head (m)
h = relative tank head (–)
n = Manning's roughness coefficient ($s\,m^{-1/3}$)
P = wet perimeter (m)
p = dimensionless wet perimeter (–)
Q = flow rate coming from upstream ($dm^3\,s^{-1}$)
Q^*_{max} = maximum flow rate causing smooth pressurization ($dm^3\,s^{-1}$)
$Q_{max,H}$ = maximum flow rate causing the tank head to be equal to H ($dm^3\,s^{-1}$)
Q_s = flow rate downstream of the jump ($dm^3\,s^{-1}$)
Q_{out} = flow rate discharged from the tank ($dm^3\,s^{-1}$)
q = dimensionless flow rate Q (–)
$q_{l,c}$ = dimensionless flow rate for which the limit curve intersects the critical-flow curve (–)
q^*_{max} = dimensionless maximum flow rate causing smooth pressurization (–)
$q_{max,h}$ = dimensionless maximum flow rate causing the relative tank head to be equal to h (–)
q_{out} = dimensionless flow rate discharged from the tank (–)
R = hydraulic radius (m)
r = dimensionless hydraulic radius (–)
S_0 = pipe slope (–)
V = flow velocity ($m\,s^{-1}$)
V_1 = free-surface flow velocity ($m\,s^{-1}$)
V_2 = flow velocity downstream of the jump ($m\,s^{-1}$)
V_{70} = flow velocity as the filling ratio is 70% ($m\,s^{-1}$)
v = dimensionless velocity (–)
v_1 = dimensionless velocity V_1 (–)
v_2 = dimensionless velocity V_2 (–)
w = wave celerity ($m\,s^{-1}$)
y_1 = free-surface flow depth (m)
$y^*_{1,max}$ = free-surface flow depth relating to the flow rate Q^*_{max} (m)
y_2 = flow depth downstream of the jump (m)
y_c = critical depth (m)
y_{G1} = centroid pressure head in Section 1 (m)
y_{G2} = centroid pressure head in Section 2 (m)
α = semi-central angle as the flow depth is y (rad)
η = filling ratio (–)
η_G = dimensionless centroid pressure head (–)
η_{G1} = dimensionless centroid pressure head in Section 1 (–)
η_{G2} = dimensionless centroid pressure head in Section 2 (–)
η_1 = filling ratio in Section 1 (–)
$\eta^*_{1,max}$ = filling ratio in Section 1 relating to the flow rate q^*_{max} (–)
$\eta_{1,max,h}$ = filling ratio in Section 1 relating to the flow rate $q_{max,h}$ (–)
θ = $S_0^{1/2}$ to ν ratio (–)
ν = dimensionless Manning's coefficient (–)
Σ = tank horizontal section (m^{-2})
ψ = Q_{out} to Q ratio (–)

References

Capart, H., Sillen, X., Zech, Y. (1997). Numerical and experimental water transients in sewer pipes. *J. Hydraulic Res.* 35(5), 659–670.

Cardle, J.A., Song, C.C.S., Yuan, M. (1989). Measurement of mixed transient flows. *J. Hydraulics Div.* 115(2), 169–182.

Ciraolo, G., Ferreri, G.B. (2008a). Sewer pressurization modelling by a rigid-column method. Proc. 11th Int. Conf. *Urban drainage* (11th *ICUD*), Edinburgh, UK, http://www.11icud.org/, on CD-ROM, 1-10.

Ciraolo, G., Ferreri, G.B. (2008b). Mathematical modelling of pressure oscillations in sewer pressurization. Proc. 11th Int. Conf. *Urban drainage* (11th *ICUD*), Edinburgh, UK, http://www.11icud.org/, on CD-ROM, 1-10.

Ferreri, G.B., Freni, G., Tomaselli, P.D. (2010). Ability of Preissmann slot scheme to simulate smooth pressurization transient in sewers. *Water Sci. Technol.* 62(8), 1848–1858.

Ferreri, G.B., Ciraolo, G., Lo Re, C. (2014). Storm sewer pressurization transient – An experimental investigation. *J. Hydraulic Res*. 52.

Guo, Q., Song, C.C.S. (1990). Surging in urban storm drainage systems. *J. Hydraulic Eng.* 116(12), 1523–1537.

Guo, Q., Song, C.C.S. (1991). Dropshaft hydrodynamics under transient conditions. *J. Hydraulic Eng.* 117(8), 1042–1055.

Hamam, M.A., McCorquodale, J.A. (1982). Transient conditions in the transition from gravity to surcharged sewer flow. *Can. J. Civil Eng.* 9(2), 189–196.

Trajkovic, B., Ivetic, M., Calomino, F., D'Ippolito, A. (1999). Investigation of transition from free surface to pressurized flow in a circular pipe. *Water Sci. Technol.* 39(9), 105–112.

Vasconcelos, J.G., Wright, S.J. (2005). Experimental investigation of surges in a stormwater storage tunnel. *J. Hydraulic Eng.* 131(10), 853–861.

Zhou, F., Hicks, F.E., Steffler, P.M. (2002a). Transient flow in a rapidly filling horizontal pipe containing trapped air. *J. Hydraulic Eng.* 128(6), 625–634.

Zhou, F., Hicks, F.E., Steffler, P.M. (2002b). Observations of air–water interaction in a rapidly filling horizontal pipe. *J. Hydraulic Eng.* 128(6), 635–639.